ARD Online First, published on September 8, 2005 as 10.1136/ard.2004.035246

THERMAL SIGNATURE ANALYSIS AS A NOVEL METHOD FOR EVALUATING INFLAMMATORY ARTHRITIS ACTIVITY.

EXTENDED REPORT

Max Brenner[*], Chris Braun[#], Mike Oster[#], Pércio S. Gulko[*].

*The Robert S. Boas Center for Genomics and Human Genetics, North Shore-LIJ Research Institute, Manhasset, NY 11030; [#]Seahorse Bioscience, Inc., North Billerica, MA, 01862.

Corresponding address:
Pércio S. Gulko M.D.
The Robert S. Boas Center for Genomics and Human Genetics
North Shore-LIJ Research Institute
350 Community Drive
Manhasset, NY
11030 – USA
Phone (516) 562-1275
FAX (516) 562-1153
Email pgulko@nshs.edu

ABSTRACT

Objectives: To determine the potential usefulness of a novel thermal imaging technology to evaluate and monitor inflammatory arthritis activity in small joints using rat models, and to determine whether thermal changes can be used to detect pre-clinical stages of synovitis.
Methods: Three different rat strains were studied in a monoarticular model of inflammatory arthritis of the ankle induced with an intra-articular (IA) injection of complete Freund's adjuvant (CFA), and compared with the contra-lateral ankle injected with normal saline. Arthritis activity and severity scores, ankle diameters, pain related posture scores, and thermal images were obtained at ten different time-points between 0h (before induction) and day 7. The pristane-induced arthritis (PIA) model was used to study pre-clinical synovitis. Thermal images were obtained at each time-point using the TSA ImagIR System and digitally analyzed.
Results: Rats developed similar ankle arthritis detected 6h after the IA injection of CFA, which persisted for seven days. All ankle clinical parameters, including arthritis activity and severity scores, significantly correlated with ankle thermal imaging changes in the monoarthritis model ($P<0.003$). No thermal imaging changes were detected in pre-clinical stages of PIA. However, PIA onset coincided with increased ankle thermal signature.
Conclusion: Thermal measurements significantly correlated with arthritis activity and severity parameters. This technology was highly sensitive and could directly measure two cardinal signs of inflammation (warmth and edema – based on ankle diameter) in an area (ankle) that is less than half the size of a human interphalangeal joint, suggesting a potential use to monitor drug responses of rheumatoid arthritis in drug trials or clinical practice.

KEYWORDS – autoimmunity, inflammation, rodent models, innate immunity, rheumatoid.

INTRODUCTION

Rheumatoid arthritis (RA) activity and severity in clinical practice and in drug trials are typically evaluated with composite scoring systems such as those developed by the American College of Rheumatology (ACR) [1], Paulus et al. [2], and Prevoo et al. (the disease activity score, DAS) [3]. These arthritis scoring systems include laboratory parameters such as levels of C-reactive protein and the erythrocyte sedimentation rate, global physician and patient assessment of disease, and investigator-dependent scorings of the number (and degree) of swollen and tender joints. While standardized, these clinical scoring systems have obvious inter-reader variability. An objective and consistent imaging technology would be very helpful for more consistent inter-institutional prospective evaluations of arthritis activity changes in drug trials, as well as in clinical practice.

There is histologic evidence of synovitis prior to the onset of clinical arthritis both in RA in humans [4], as well as collagen- [5], and pristane-induced arthritis [6] (Brenner et al. unpublished observations) in rats (CIA and PIA, respectively). Studying synovial tissue obtained at these pre-clinical stages during disease development has the potential of identifying novel pathways involved in disease pathogenesis. However, there are no objective parameters to determine which joints have pre-clinical synovitis in order to guide closed-needle or arthroscopic synovial biopsies for functional or gene expression studies.

Available imaging technologies such as magnetic resonance imaging (MRI) [7-10] and scintigraphy [8, 11, 12] can detect inflammation and joint swelling but are expensive and not practical for repetitive use. Additionally, synovitis-like changes have been described in up to 9% of normal metacarpophalangeal joints studied with MRI [13], and the specificity of those findings remains to be determined. The use of articular ultrasound appears promising in the presence of joint swelling [8-10, 14], but it has not been studied in pre-clinical synovitis. Additionally, articular ultrasonography is highly reader-dependent and has not yet been standardized.

Warmth is a cardinal feature of inflammation and may be objectively measured by the use of infra-red-based thermography [15]. Several studies have demonstrated good correlation between thermographic findings and disease activity indexes in large joints, but not in small joints [16-18] of patients with RA, thus limiting the potential usefulness of these technologies in clinical trials or office practice. However, recent advancements both in infra-red imaging and analytical technologies now allow for more precise temperature measurements in smaller surface areas.

We were interested in identifying novel and convenient imaging methods to evaluate and monitor inflammation in RA joints as an objective parameter to measure disease activity for use in both drug trials as well as in clinical practice. Moreover, we are interested in identifying non-invasive methods to detect the very early pre-clinical stages during the pathogenesis of arthritis. Therefore, we designed this pilot study in rats to test whether a novel thermal imaging system could be a useful tool to evaluate disease activity (and arthritis severity) in a surface area that is smaller than a typical human proximal interphalangeal joint (rat ankles), and whether the thermal

signature could serve as a biomarker for pre-clinical synovitis. Two rat models of arthritis were used in these studies.

MATERIAL AND METHODS

Rats – Eight to twelve week-old female DA, ACI and F344 rats were purchased from Harlan (Indianapolis, IN) and used in all experiments. All the work done with rats was reviewed and approved by the North Shore-LIJ Research Institute Institutional Animal Care and Use Committee.

Monoarthritis model

Induction of monoarthritis **-** This is a localized model of arthritis that begins within 2-6h after the induction. This model was used to study the correlation between arthritis activity/severity and the thermal imaging data. Each rat received a single intra-articular left ankle injection of 40μL of a mixture of Complete Freund's Adjuvant (CFA, Difco) mixed with normal saline at 1:1 [19, 20], and compared with a saline injection on the right ankle.

Scoring parameters used in the monoarthritis model

All parameters below were acquired at time 0h, 6h, 12h, 24h, and then once a day, until day 7.

a. Bilateral ankle diameters (latero-lateral and antero-posterior): Diameters were measured with a digital caliper to the nearest 100th of a millimeter (Fisher Scientific).
b. Clinical arthritis activity/severity scoring system: Both ankles and midfoot joints were scored ranging from 0-4 according to joint size and ability to support weight, where 0=no joint swelling, 1=mild swelling, 2=moderate swelling, 3=severe (maximal) swelling, 4=severe swelling plus non-weight bearing. This is an ankle and midfoot-focused version of a scoring system described in details below, and commonly used to evaluate systemic autoimmune arthritis [21-23].
c. Pain-related posture (PRP): The posture of each animal's hindlimb was scored according to a pain-related behavioral scale (spontaneous pain rating score) (0-5) 0=normal; 1=curling of the toes; 2=eversion of the paw; 3=partial weight bearing; 4=non-weight bearing and guarding; and 5=avoidance of any contact with the hindlimb [24].

Systemic autoimmune arthritis model (Pristane-induced arthritis, PIA)

Induction of PIA – PIA is a model of systemic autoimmune arthritis with disease onset typically 14 days following induction. DA rats are highly susceptible to PIA, with an incidence of arthritis of nearly 100%. Because of this predictable course, PIA was used to determine whether thermal imaging signature changes occurred prior to the onset of clinical disease, reflecting pre-clinical synovitis, and whether those changes could be useful markers to predict histologic findings. DA rats were injected with 150μl of pristane (2,6,10,14-tetramethylpentadecane, SIGMA-Aldrich Chemical Co., Milwaukee, WI) [6, 25]. The dose was divided into two intradermal injections at the base of the tail.

Scoring of systemic polyarticular arthritis - Rats were scored daily between days 0-16 according to a well-established scoring system [21-23]. Specifically, the arthritis scoring system evaluates individual joints, and weights the arthritis severity by joint size as follows: a) wrist, mid forepaw, ankle and midfoot joints were scored 0 to 4 as follows: 0=no swelling; 1=mild swelling; 2=moderate swelling; 3=severe swelling; 4=severe swelling and non-weight bearing; b) presence of arthritis in each of the 3 joints in the 2nd to 5th digits (2 interphalangeal plus

metatarsophalangeal or metacarpophalangeal joints): 0=swelling absent; 1=swelling present. The total score for each extremity was calculated by adding the scores of the individual joints. The maximum score for each extremity is, therefore, 20, and the maximum total joint score per rat is 80.

Thermal imaging acquisition and digital analyses

The Seahorse Bioscience TSA ImagIR Thermal Imaging system (Seahorse Bioscience, N. Billerica, MA) was used in accordance with the manufacturer's procedures to image rats at every time point (figure 1A). The TSA ImagIR employs a platinum silicide 256x256 pixel detector array filtered to be sensitive to infra-red (IR) radiation in the 3-5μm wavelength. This sensor returns signals to the processor that are proportional to the photons of IR radiation detected. These data, combined with thermal reference devices allow the instrument to detect the temperatures of all objects in the field of view simultaneously and in real time [26, 27].

Rats received anesthesia induction in a sealed acrylic chamber via administration of 5% isoflurane in oxygen flowing at 2L/minute for approximately 1 minute. Following induction, rats were transferred from the acrylic induction chamber to the ImagIR imaging chamber's temperature controlled anesthesia delivery module, where they received 2-3% maintenance isoflurane in oxygen. Rats' body temperatures were maintained between 36-37°C using a temperature controlled imaging platform with a constant temperature of 35°C (accurate to $\pm$0.1°C). Legs were positioned in flexion and external rotation to expose the medial part of each ankle to the infrared sensor (figure 1B and 1C). Rats were imaged for a total of 10 minutes capturing images every 15 seconds. Each captured image was generated by averaging 16 frames of video rate image data together to produce a clear still image. Both anesthesia and the thermal imaging acquisition were done in a room with a constant temperature of 21-23°C.

The thermal imaging data were extracted from saved images using Animal Corral Software version 4.0.0 (Seahorse Bioscience, N. Billerica, MA). First, a region of interest (ROI) was drawn to delineate left and right ankles. The typical limits for the ROI were the ankle fur line (upper limit) and the midfeet's midpoint. The average temperature of all pixels within each ROI in each image was calculated and recorded automatically. Data quality at the beginning of each 10 minutes imaging period was similar to that obtained at the middle and end of each imaging period. Additionally, it was determined that the initial images better reflected pre-anesthesia body and ankle temperatures (data not shown). Therefore, only data from the initial images were used, making the time to image each animal less than one minute, thus minimizing any anesthetic-induced effect in body temperature regulation.

Thermal images were obtained at 0h (pre-injection), 6h, 12h, 24h, and daily on days 2-7 after intra-articular CFA (or saline) administration (monoarthritis model), and daily from day 0 to day 16 in PIA. In order to correct for each individual rat's own peripheral limb temperature, left ankle (CFA) thermal measurements were corrected for the right ankle (saline) measurements (left ankle minus right ankle) in the monoarthritis studies. In PIA, since both ankles are typically involved, thermal measurements were adjusted for the core-temperature obtained with a rectal probe.

Histology and histologic scoring.
Hind paws were fixed in 10% formaldehyde at the end of the monoarthritis observation period (day 7). Rats studied for PIA were euthanized on days 7, 11 and 16 (four rats per time-point), and their hind paws fixed as described above. Paws were then decalcified with a solution containing hydrochloric acid and 0.1M EDTA (Cal-Ex, Fisher Scientific, Fairlawn, NJ). Tissues were embedded in paraffin, sectioned and stained with hematoxylin-eosin. We used a recently described comprehensive histologic scoring system [28, 29]. Briefly, tibio-talar, talus-calcaneal and midfoot joints were histologically scored for the following parameters:

1. Synovial inflammation. Five high-power magnification fields (HMF) were scored for the percentage of infiltrating mononuclear cells as follows: 0=absent; 1=mild (1-10%); 2=moderate (11-50%); 3=severe (51-100%). The mean of the five HMF was used for analysis.
2. Synovial hyperplasia. 0=absent; 1=mild (5-10 layers); 2=moderate (11-20 layers); 3=severe (>20 layers).
3. Extension of pannus formation based on the reader's impression. 0=absent; 1=mild; 2=moderate; 3=severe.
4. Synovial fibrosis. 0=absent; 1=mild (1-10%); 2=moderate (11-50%); 3=severe (51-100%).
5. Synovial vascularity (angiogenesis). The number of vessels was counted in five HMF of synovial tissue, and the mean used for analysis.
6. Cartilage erosions. Percentage of the cartilage surface that was eroded: 0=absent; 1=mild (1-10%); 2=moderate (11-50%); 3=severe (51-100%).
7. Bone erosions. 0=none; 1=minor (observed only at HMF); 2=moderate (observed at low magnification); 3=severe (transcortical).

Statistical analyses
Medians were compared with the Mann-Whitney rank sum test or with ANOVA on ranks with a pairwise multiple comparison procedure (Dunn's method). Variables were correlated with the Pearson's correlation coefficient. A *P* value of 0.05 or less was regarded as significant. All statistical analyses were done with SigmaStat 3.0 (SPSS, Chicago, IL).

RESULTS

Thermal imaging signature correlated with arthritis clinical activity and severity in the monoarthritis model – All DA, ACI and F344 rats injected intra-articularly with CFA developed similar clinical monoarthritis which was detectable at 6h post-injection and reached its peak between days 1 and 3 (figure 2A). The arthritis scores of these three strains were not significantly different in any of the studied time-points (figure 2A). None of the rats developed arthritis in the saline-injected joints.

Left ankle thermal imaging readings (arthritic) were adjusted for the right ankle thermal readings (non-arthritic) for each individual rat (left minus right). Non-adjusted and adjusted temperatures consistently increased in arthritic ankles in all three strains (figure 2B). DA and F344 temperatures increased significantly more than ACI rats' temperatures from 12h (0.5 day) until day 3 (figure 2B). DA and ACI thermal readings remained significantly different from day 5 to day 7. These inter-strain arthritic ankles' temperature variations did not translate into differences

in arthritis activity and severity scores (figure 2A), or into differences in synovial inflammatory infiltration, synovial hyperplasia, synovial vascularization, nor cartilage and bone erosions (table I).

The thermal imaging readings were significantly correlated with the arthritis activity and severity clinical scores, joint diameter, and PRP clinical scores ($P<0.001$, Pearson's correlation coefficient matrix, table II).

Thermal imaging signature did not change in pre-clinical stages in PIA – We studied PIA in 12 female DA rats in order to determine whether daily thermal imaging readings changed in pre-clinical stages, and whether those changes could predict histologic abnormalities. Groups of four rats were euthanised on days 7, 11 and 16 after the induction of PIA, and their paws prepared for histology. While histologic abnormalities were detectable at day 11 post-induction, including inflammatory infiltration and synovial hyperplasia, the thermal signature did not significantly change before the onset of clinical arthritis (data not shown).

Thermal imaging signature correlated with arthritis severity scores in the PIA – Four rats used in the 'pre-clinical stage' experiment described above with PIA developed clinical evidence of ankle arthritis between days 10 and 16. Despite the small number of rats there was a strong correlation between ankle arthritis scores and thermal signatures ($P<0.001$).

DISCUSSION

We were interested in identifying novel, convenient, non-invasive and inexpensive imaging methods to quantify joint inflammation in RA. New infrared-based technologies that allow for a more precise quantification of temperature variations in small surface areas, such as the interphalangeal joints, appeared promising. While older versions of infra-red based thermographic analyses have been previously used to evaluate RA activity, none of those studies could reliably assess the hand joints, and typically the analyses were limited to knees, elbows, and wrists [16-18]. In the present study we used a highly sensitive thermal imaging system that could reproducibly detect temperature variations in the rat ankle joint, an area that is less than half the size of a human proximal interphalangeal joint. Moreover, thermal variations correlated well with well-established rodent clinical arthritis activity and severity scores, as well as with changes in the articular diameter and pain posture in a monoarthritis model. Thermal imaging could also be used to measure joint diameter as an indicator of joint swelling/edema (data not shown). These results suggest that the novel thermal imaging technologies could provide useful and objective measurements of joint inflammation based on two cardinal inflammatory signs, namely joint swelling/edema (joint diameters) and warmth. The objective and prospective thermal imaging documentation could be helpful in drug trials as well as in clinical practice.

All three strains developed significant and similar histologic abnormalities, demonstrating that changes in thermal signature predicted increased histologic severity. There were inter-strain variations in the magnitude of the thermal signature variation, with ACI rats having a less pronounced thermal elevation compared with DA and F344. Still, there was a significant correlation between the thermal signature and clinical disease severity in all three strains. The

inter-strain difference in the magnitude of the thermal variations did not translate into significant clinical or histologic differences in arthritis severity and its relevance remains to be determined.

We were also interested in studying very early stages in the pathogenesis of synovitis and wanted to determine whether the thermal imaging analyses could identify pre-clinical stages of synovitis. The rapid and abrupt onset of arthritis in the monoarthritis model following the intra-articular injection of CFA does not allow any time for the development of pre-clinical synovitis. Therefore, we chose to study a systemic model of autoimmune arthritis, PIA, known to typically develop over a 14-day period. Ankle thermal signature elevations were detected after the onset of clinical disease, but not prior to it. Ankle thermal signatures correlated with clinical arthritis severity scores.

Histologic analyses of ankle joints obtained from rats with PIA have demonstrated that synovial hyperplasia, synovial infiltration with mononuclear cells, and fibrin deposition can be detected in the synovial tissues around day 11, before the onset of clinical disease [6], and that increased numbers of neutrophils are present around the time of disease onset (Brenner et al., unpublished observations). However, the early pre-clinical histologic abnormalities did not correlate with any thermal imaging signature changes (data not shown). The association of disease onset with increased numbers of neutrophils in the synovial fluid and tissue in PIA suggests that these cells and their products are directly or indirectly central to the regulation of the articular thermal signature. As a result, thermal signature analysis did not appear to be helpful in detecting pre-clinical stages of synovitis.

In conclusion, the new generation of thermal imaging technologies has significantly improved resolution and temperature-sensitivity, and generates reproducible measurements of surface areas smaller than an interphalangeal joint. We consider that this novel, less reader-dependent and non-invasive technology has the potential to become a useful and objective tool for measuring inflammatory arthritis activity, and for generating digital data that can be stored and analyzed both in drug trials as well as in office-based clinical practice.

AKNOWLEDGEMENTS

This study was funded in part by the Seahorse Bioscience, Inc.

REFERENCES

1. DT Felson, JJ Anderson, M Boers, C Bombardier, D Furst, C Goldsmith, LM Katz, R Lightfoot, Jr., H Paulus, V Strand, et al: **American College of Rheumatology. Preliminary definition of improvement in rheumatoid arthritis**. *Arthritis Rheum* 1995, **38**:727-35.
2. HE Paulus, MJ Egger, JR Ward, HJ Williams: **Analysis of improvement in individual rheumatoid arthritis patients treated with disease-modifying antirheumatic drugs, based on the findings in patients treated with placebo. The Cooperative Systematic Studies of Rheumatic Diseases Group**. *Arthritis Rheum* 1990, **33**:477-84.
3. ML Prevoo, MA van 't Hof, HH Kuper, MA van Leeuwen, LB van de Putte, PL van Riel: **Modified disease activity scores that include twenty-eight-joint counts. Development**

and validation in a prospective longitudinal study of patients with rheumatoid arthritis. *Arthritis Rheum* 1995, **38**:44-8.
4. JA Pando, P Duray, C Yarboro, MF Gourley, JH Klippel, HR Schumacher: **Synovitis occurs in some clinically normal and asymptomatic joints in patients with early arthritis**. *J Rheumatol* 2000, **27**:1848-54.
5. JP Caulfield, A Hein, R Dynesius-Trentham, DE Trentham: **Morphologic demonstration of two stages in the development of type II collagen-induced arthritis**. *Lab Invest* 1982, **46**:321-43.
6. C Vingsbo, P Sahlstrand, J Brun, R Jonsson, T Saxne, R Holmdahl: **Pristane-induced arthritis in rats: A new model for rheumatoid arthritis with a chronic disease course influenced by both major histocompatibility complex and non-major histocompatibility complex genes.** *Am J Pathol* 1996, **149**:1675-1683.
7. P Goupille, B Roulot, S Akoka, AM Avimadje, P Garaud, L Naccache, A Le Pape, JP Valat: **Magnetic resonance imaging: a valuable method for the detection of synovial inflammation in rheumatoid arthritis**. *J Rheumatol* 2001, **28**:35-40.
8. M Backhaus, T Kamradt, D Sandrock, D Loreck, J Fritz, KJ Wolf, H Raber, B Hamm, GR Burmester, M Bollow: **Arthritis of the finger joints: a comprehensive approach comparing conventional radiography, scintigraphy, ultrasound, and contrast-enhanced magnetic resonance imaging**. *Arthritis Rheum* 1999, **42**:1232-45.
9. M Szkudlarek, E Narvestad, M Klarlund, M Court-Payen, HS Thomsen, M Ostergaard: **Ultrasonography of the metatarsophalangeal joints in rheumatoid arthritis: comparison with magnetic resonance imaging, conventional radiography, and clinical examination**. *Arthritis Rheum* 2004, **50**:2103-12.
10. JL Hoving, R Buchbinder, S Hall, G Lawler, P Coombs, S McNealy, P Bird, D Connell: **A comparison of magnetic resonance imaging, sonography, and radiography of the hand in patients with early rheumatoid arthritis**. *J Rheumatol* 2004, **31**:663-75.
11. F Jamar, DH Manicourt, N Leners, M Vanden Berghe, C Beckers: **Evaluation of disease activity in rheumatoid arthritis and other arthritides using 99mtechnetium labeled nonspecific human immunoglobulin**. *J Rheumatol* 1995, **22**:850-4.
12. MH de Bois, PP Tak, JW Arndt, PM Kluin, EK Pauwels, FC Breedveld: **Joint scintigraphy for quantification of synovitis with 99mTc-labelled human immunoglobulin G compared to histological examination**. *Clin Exp Rheumatol* 1995, **13**:155-9.
13. B Ejbjerg, E Narvestad, E Rostrup, M Szkudlarek, S Jacobsen, HS Thomsen, M Ostergaard: **Magnetic resonance imaging of wrist and finger joints in healthy subjects occasionally shows changes resembling erosions and synovitis as seen in rheumatoid arthritis**. *Arthritis Rheum* 2004, **50**:1097-106.
14. TM Spiegel, W King, 3rd, SR Weiner, HE Paulus: **Measuring disease activity: comparison of joint tenderness, swelling, and ultrasonography in rheumatoid arthritis**. *Arthritis Rheum* 1987, **30**:1283-8.
15. EF Ring: **The historical development of thermal imaging in medicine**. *Rheumatology (Oxford)* 2004, **43**:800-2.
16. MD Devereaux, GR Parr, DP Thomas, BL Hazleman: **Disease activity indexes in rheumatoid arthritis; a prospective, comparative study with thermography**. *Ann Rheum Dis* 1985, **44**:434-7.

17. C Rajapakse, DM Grennan, C Jones, L Wilkinson, M Jayson: **Thermography in the assessment of peripheral joint inflammation--a re-evaluation**. *Rheumatol Rehabil* 1981, **20**:81-7.
18. F Singer, J Gruber, J Graber, M Reinthaler, N Thumb: **The use of thermography in the evaluation of the anti-inflammatory activity of feprazone on rheumatoid arthritis**. *Arzneimittelforschung* 1982, **32**:427-9.
19. T Pelissier, A Hernandez, C Mestre, A Eschalier, C Laurido, C Paeile, P Alvarez, R Soto-Moyano: **Antinociceptive effect of clomipramine in monoarthritic rats as revealed by the paw pressure test and the C-fiber-evoked reflex**. *Eur J Pharmacol* 2001, **416**:51-7.
20. S Yoshino, J Yoshino: **Recruitment of pathogenic T cells to synovial tissues of rats injected intraarticularly with nonspecific agents**. *Cell Immunol* 1994, **158**:305-13.
21. PS Gulko, Y Kawahito, EF Remmers, VR Reese, J Wang, SV Dracheva, L Ge, RE Longman, JS Shepard, GW Cannon, et al: **Identification of a new non-major histocompatibility complex genetic locus on chromosome 2 that controls disease severity in collagen- induced arthritis in rats.** *Arthrititis Rheum* 1998, **41**:2122-31.
22. Y Kawahito, G Cannon, P Gulko, E Remmers, R Longman, V Reese, J Wang, M Griffiths, R Wilder: **Localization of quantitative trait loci regulating adjuvant induced arthritis in rats: evidence for genetic factors common to multiple autoimmune diseases.** *J Immunol* 1998, **161**:4411-9.
23. H Meng, M Griffiths, E Remmers, Y Kawahito, W Li, R Neisa, R Cannon, R Wilder, P Gulko: **Identification of two novel female-specific non-MHC loci regulating collagen-induced arthritis severity and chronicity, and evidence of epistasis.** *Arthritis Rheum* 2004, **50**:2695-705.
24. L Zhang, Y Lu, Y Chen, KN Westlund: **Group I metabotropic glutamate receptor antagonists block secondary thermal hyperalgesia in rats with knee joint inflammation**. *J Pharmacol Exp Ther* 2002, **300**:149-56.
25. EF Remmers, B Joe, MM Griffiths, DE Dobbins, SV Dracheva, A Hashiramoto, T Furuya, JL Salstrom, J Wang, PS Gulko, et al: **Modulation of multiple experimental arthritis models by collagen-induced arthritis quantitative trait loci isolated in congenic rat lines: different effects of non-major histocompatibility complex quantitative trait loci in males and females**. *Arthritis Rheum* 2002, **46**:2225-34.
26. MA Paulik, RG Buckholz, ME Lancaster, WS Dallas, EA Hull-Ryde, JE Weiel, JM Lenhard: **Development of infrared imaging to measure thermogenesis in cell culture: thermogenic effects of uncoupling protein-2, troglitazone, and beta-adrenoceptor agonists**. *Pharm Res* 1998, **15**:944-9.
27. RA Koza, K Flurkey, DM Graunke, C Braun, HJ Pan, PC Reifsnyder, LP Kozak, EH Leiter: **Contributions of dysregulated energy metabolism to type 2 diabetes development in NZO/H1Lt mice with polygenic obesity**. *Metabolism* 2004, **53**:799-808.
28. M Brenner, H Meng, N Yarlett, M Griffiths, E Remmers, R Wilder, P Gulko: **The non-MHC quantitative trait locus Cia10 contains a major arthritis gene and regulates disease severity, pannus formation and joint damage.** *Arthritis Rheum.* 2005, **52**:322-32.
29. M Brenner, HC Meng, NC Yarlett, B Joe, MM Griffiths, EF Remmers, RL Wilder, PS Gulko: **The Non-MHC Quantitative Trait Locus Cia5 Contains Three Major Arthritis Genes That Differentially Regulate Disease Severity, Pannus Formation,**

and Joint Damage in Collagen- and Pristane-Induced Arthritis. *J Immunol* 2005, **174**:7894-903.

FIGURE LEGENDS

Figure 1. Thermal imaging work station and monoarthritis rats. **A.** Work station with anesthesia chamber (ac) and thermal imager acquisition station (as). The open compartment has a sliding platform where anesthetized rats are positioned for image acquisition. **B.** Rat with left ankle CFA-induced monoarthritis (arrowhead) and normal saline-injected right ankle. **C.** Thermogenic image of a rat with left monoarthritis revealing increased temperature (bright yellow region labeled '2') while the saline-injected right ankle has a temperature that is not different than that of the tail.

Figure 2. Arthritis activity and severity scores and thermogenic images in the monoarthritis model during a seven day observation period. **A.** Arthritis scores (mean±SEM) of the left ankle of the three strains. Medians were compared with ANOVA on ranks. There were no significant differences between the three strains. **B.** Temperature (in degrees Celsius, °C) in DA, ACI, and F344 left (CFA injected) minus right (saline injected) ankles (mean±SEM) during the seven-day observation period. Median temperature changes were compared among strains with ANOVA on ranks, and a $P<0.05$ was regarded as significant. * =significant difference between ACI and DA, and between ACI and F344; ** =significant difference between ACI and F344 only; #=significant difference between ACI and DA only.

Table I: Histologic scores of left ankles collected 7 days after CFA injection.

	DA (n=5)	F344 (n=5)	ACI (n=5)
Inflammatory infiltrate (0-3)	2.04 ± 0.35	2.56 ± 0.17	2.52 ± 0.16
Synovial hyperplasia (0-3)	1.40 ± 0.68	2.60 ± 0.24	2.60 ± 0.40
Pannus (0-3)	2.00 ± 0.32	1.40 ± 0.24	2.00 ± 0.32
Fibrosis (0-3)	0.80 ± 0.37	0.00 ± 0.00	0.00 ± 0.00
Vessels / HMF	7.28 ± 1.28	7.60 ± 2.37	8.80 ± 2.09
Cartilage erosions (0-3)	0.60 ± 0.40	1.20 ± 0.20	1.20 ± 0.20
Bone erosions (0-3)	1.40 ± 0.60	1.80 ± 0.37	2.20 ± 0.37

5 rats per strain were randomly selected for histologic analysis.
Values are means ± standard error of the mean. Differences were not statistically significant.

Table II. Pearson's correlation coefficient matrix relating thermal signature and clinical parameters in the intra-articular CFA monoarthritis model (left ankle)*.

		arthritis activity and severity score		left limb PRP	ankle diameters	
		left ankle	L ankle+L midfoot#		lateral, left-right	AP, left-right
ankle temperature (left-right)	*r*	0.602	0.597	0.522	0.643	0.569
	P	0.000427	0.000502	0.00309	0.000128	0.00104
left ankle arthritis activity and severity score	*r*		0.985	0.834	0.908	0.902
	P		4.16×10^{-23}	1×10^{-8}	4.47×10^{-12}	1×10^{-11}
left ankle+left midfoot arthritis activity & severity score	*r*			0.875	0.857	0.898
	P			2.63×10^{-10}	1.5×10^{-9}	1.7×1011^{-11}
left limb pain related posture (PRP)	*r*				0.687	0.819
	P				0.0000272	3×1011^{-8}
ankle lateral diameter (left-right)	*r*					0.892
	P					3.9×10^{-11}

* n=30 (10 rats per strain). Correlation results include two values: 'r' correlation coefficient and the 'P' value.
PRP=pain-related posture; left-right=left minus right (see text for definitions).
Data from ten different time-points (day 0, 6h, 12h, 24h, and days 2-7) were included in these analyses.
L=left.

Figure 1

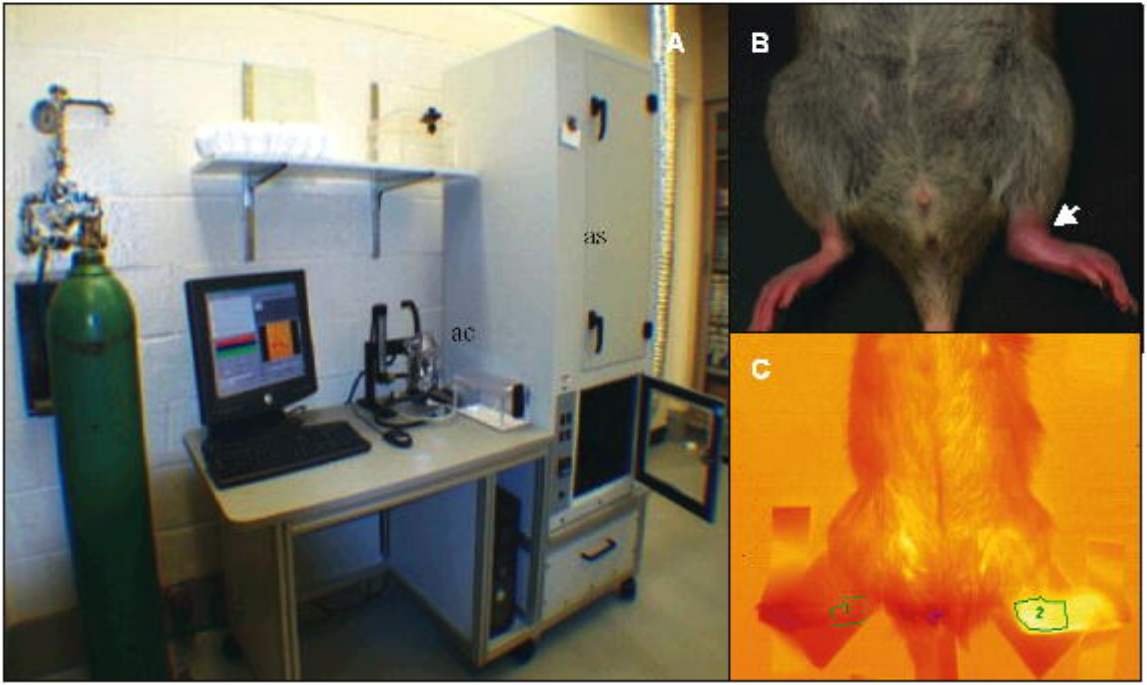

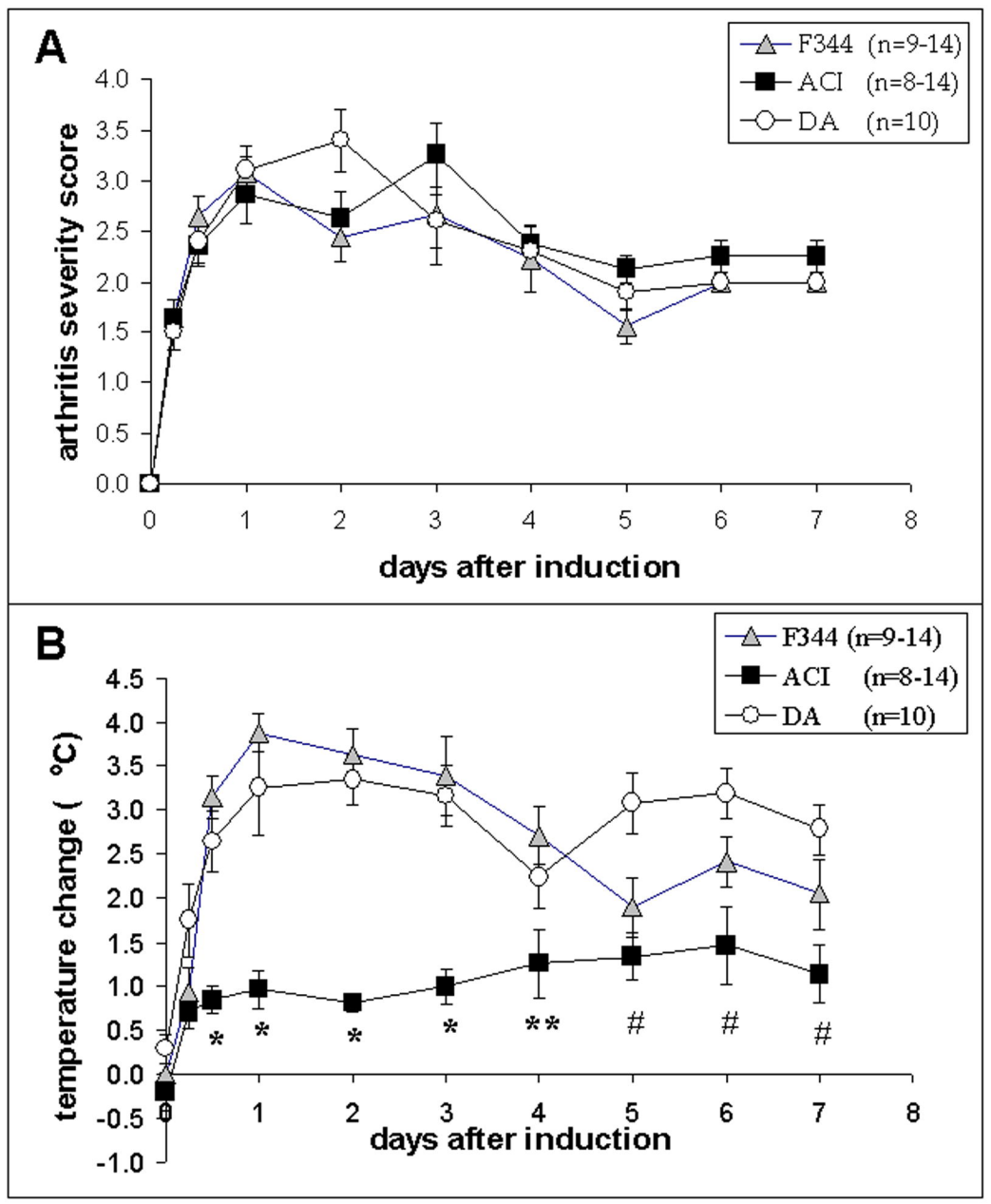
A
F344 (n=9-14)
ACI (n=8-14)
DA (n=10)
arthritis severity score
4.0
3.5
3.0
2.5
2.0
1.5
1.0
0.5
0.0
0
1
2
3
4
5
6
7
8
days after induction
B
F344 (n=9-14)
ACI (n=8-14)
DA (n=10)
temperature change (°C)
4.5
4.0
3.5
3.0
2.5
2.0
1.5
1.0
0.5
0.0
-0.5
-1.0
*
*
*
*
**
#
#
#
0
1
2
3
4
5
6
7
8
days after induction